

## Electronic Supplementary Information

### **Synthesis of amphiphilic graphitic silver nanoparticles with inherent internal standard: an efficient strategy for reliable quantitative SERS analysis in common fluids**

Zhi-Ling Song,<sup>a</sup> Xin Dai,<sup>a</sup> Mengru Li,<sup>a</sup> Zhen Song,<sup>a</sup> Zhuo Chen,<sup>\*b</sup> Xiliang Luo<sup>\*a</sup>

<sup>a</sup> *Key Laboratory of Sensor Analysis of Tumor Marker, Ministry of Education, College of Chemistry and Molecular Engineering, Qingdao University of Science and Technology, Qingdao 266042, P. R. China.*

*Email: xiliangluo@qust.edu.cn*

<sup>b</sup> *Molecular Science and Biomedicine Laboratory (MBL), State Key Laboratory of Chemo/Bio-Sensing and Chemometrics, College of Chemistry and Chemical Engineering and College of Life Sciences, Aptamer Engineering Center of Hunan Province, Hunan University, Changsha Hunan, 410082(China).*

*Email: zhuochen@hnu.edu.cn*

## Table of Contents

1. Materials and reagents .....	S3
2. Synthesis of GSN.....	S3
3. Characterization of GSN.....	S4
4. Synthesis of N <sub>3</sub> -PEG .....	S4
5. Synthesis of N <sub>3</sub> -dodecane .....	S5
6. Synthesis of AGSN .....	S5
7. Characterization of AGSN .....	S6
8. Stability tests of AGSN for Raman analysis.....	S7
9. Raman analysis of AGSN as an internal standard.....	S8
10. Preparation of fish samples.....	S8
11. Raman analysis of AGSN for LMG and MG in different solvents.....	S9
Fig. S1.....	S11
Fig. S2.....	S11
Fig. S3.....	S12
Fig. S4.....	S12
Fig. S5.....	S13
Fig. S6.....	S13
Fig. S7.....	S14
Fig. S8.....	S15
Fig. S9.....	S15
References.....	S16

## 1. Materials and reagents

Hydrous copper nitrate ( $\text{CuNO}_3 \cdot 3\text{H}_2\text{O}$ ), anhydrous silver nitrate ( $\text{AgNO}_3$ ), anhydrous magnesium sulphate ( $\text{MgSO}_4$ ), sodium sulfate ( $\text{NaSO}_4$ ) and Rhodamine 6G (R6G) were obtained from Aladdin. Toluene, o-dichlorobenzene (ODCB), chloroform, dichloromethane (DCM), tetrahydrofuran (THF), acetone, acetonitrile, ethyl acetate (EtOAc), dimethyl formamide (DMF), ethanol, methanol and dimethyl sulfoxide (DMSO) were purchased from Adamas. Triethylamine ( $\text{Et}_3\text{N}$ ), methanesulfonyl chloride (MsCl), methoxy-PEG, sodium azide ( $\text{NaN}_3$ ), malachite green oxalate (MG), leucomalachite green (LMG), potassium permanganate ( $\text{KMnO}_4$ ), sodium periodate ( $\text{NaIO}_4$ ), 1-bromododecane and 2,3-dichloro-5,6-dicyano-1,4-benzoquinone (DDQ) were gained from Changsha Chemical Reagents Company (Changsha, China). Tilapia muscle was purchased from Guolian Aquatic Co., Ltd (Guangdong, China). All the other chemicals of analytical reagent grade were obtained from Changsha Chemical Reagents Company (Changsha, China) and used as received without further purification. Doubly distilled water (resistance  $> 18 \text{ M}\Omega \text{ cm}^{-1}$ ) was used throughout all experiments.

## 2. Synthesis of GSN

GSN was synthesized according to previous report of our group by chemical vapor deposition (CVD) method.<sup>S-1</sup> Briefly, fumed silica (1 g, Aladdin) was mixed with  $\text{AgNO}_3$  (152 mg) and  $\text{CuNO}_3 \cdot 3\text{H}_2\text{O}$  (70 mg) and sonicated for 1 h in methanol. Then, the ground powder was gained by drying at  $50 \text{ }^\circ\text{C}$ . Next, the powder was laid in a CVD

system to grow GSN nanoparticles at high temperature. After growth, the sample was etched with HF and HNO<sub>3</sub> to dissolve the silica and the uncovered AgCu particles. Finally, the GSN solid was obtained by washing and centrifuging several times.

### **3. Characterization of GSN**

Transmission electron microscopy (TEM, JEM-2010) was utilized to image the size and morphology. Field emission electron microscopy (G2F20 S-TWIN) was applied to characterize the scanning transmission electron microscopy (STEM) image of GSN. The energy dispersive spectrometry (EDS) was demonstrated in Fig.S1 which showed the AgCu alloy structure of GSN core. The plasmonic properties of GSN were characterized by the UV-2450 UV-vis spectrophotometer (Shimadzu).

### **4. Synthesis of N<sub>3</sub>-PEG**

N<sub>3</sub>-PEG was synthesized according to previous report.<sup>S-2</sup> O-methanesulfonyl-O-methylpolyethylene glycol (Ms-PEG) was first synthesized. Commercial methoxy-PEG (MW1000, 15.0 g, 0.015 mol, 1 eq.) and Et<sub>3</sub>N (1.97 g, 0.0195 mol, 1.3 eq.) were dissolved in dried DCM (60 mL). Then, MsCl (2.23 g, 0.0195 mol, 1.3 eq.) was added dropwise to the mixture under stirring over 15 min at 0 °C. Then the sample was stirred at 0 °C for additional 15 min, and reacted at room temperature overnight. Next, the generated heterogeneous solution was washed three times with water (3×30 mL). The resulting organic layer was filtered after drying over anhydrous Na<sub>2</sub>SO<sub>4</sub>, and the followed solvent was evaporated to get Ms-PEG. Ms-PEG (16.1 g, 0.0149 mol, 1 eq.) was then mixed with NaN<sub>3</sub> (3.9 g, 0.0594 mol, 4 eq.) in DMF (48 mL). The solution was refluxed in a round flask at 60 °C overnight and then diluted with water (50 mL)

and stirred for a further 40 min. Next, the mixture was extracted four times with DCM (4×25 mL). The combined organic layer was dried over anhydrous NaSO<sub>4</sub> followed by filtering, and the solvent was evaporated to get crude compound. Then isopropyl ether (80 mL) was added and stirred at room temperature for 30 min. Finally, N<sub>3</sub>-PEG was gained by filtering and drying.

### **5. Synthesis of N<sub>3</sub>-dodecane**

NaN<sub>3</sub> (294 mg, 4.52 mmol) and 1-bromododecane (939 mg, 3.77 mmol) were dissolved in DMSO (20 mL) successively. Then the solution was stirred at room temperature overnight. After that, water and 1 M HCl was added to dilute the solution. The resulting aqueous phase was extracted three times with EtOAc (3×15 mL). The combined organic layer was washed with water and dried over anhydrous Na<sub>2</sub>SO<sub>4</sub>, and then the solvent was evaporated to get crude compound N<sub>3</sub>-dodecane.

### **6. Synthesis of AGSN**

For the amphiphilic functionalization of GSN, the weight ratio of GSN to azides was about 1:1000. First, GSN powder was dispersed in ODCB (0.1 mg/mL, 20 mL) and sonicated for 10 min followed by preheating to 160 °C under nitrogen protection. Then 1000-fold weight excess of N<sub>3</sub>-dodecane and N<sub>3</sub>-PEG in 5 mL ODCB were added dropwise to the reaction solution over 20-30 min. Next, the temperature was maintained at 160 °C for additional 45 min, after which the mixture was cooled down to room temperature. The resulting suspension was washed with ODCB and acetone alternately to remove all the by-products and the AGSN was collected through centrifugation.

Furthermore, the synthesis of hydrophilic and lipophilic GSN were similar to the AGSN except for adding only one kind of corresponding azides.

## 7. Characterization of AGSN

The covalent functionalization of AGSN was further tested by FT-IR and Raman spectra (Fig. S2). In Fig. S2a, the absorption bands at  $\sim 2100\text{ cm}^{-1}$  of azido stretching vibration disappeared, but the absorption bands at  $\sim 1120\text{ cm}^{-1}$  of C-N stretching increased in AGSNs, which declared the new covalent bonds of C-N formed after azides converting to nitrenes and attacking the  $\text{sp}^2\text{ C}=\text{C}$  of graphitic shells. Furthermore, GSN has three prominent Raman vibration bands: a graphitic carbon (G) peak around  $1590\text{ cm}^{-1}$ , a disordered (D) peak around  $1330\text{ cm}^{-1}$  and 2D peak around  $2640\text{ cm}^{-1}$  (Fig. S2b). The relatively high Raman D peak of GSN is attributed to the defective nature and distorted  $\text{sp}^2$  bonds of graphitic shells, accompanied with the strain-induced effects and finite particle-size effects.<sup>S-3</sup> The Raman spectrum of AGSN was similar to GSN, all showed three peaks of D band, G band and 2D band, respectively (Fig. S2b). Notably, the D band intensity of AGSN slightly enhanced, because more disordered bonds emerged in the graphitic shells resulted from the addition of nitrenes to the graphitic  $\text{sp}^2\text{ C}=\text{C}$  bonds, which further illustrated the successful functionalization. The PEG and dodecane were also used to modify the nanoparticles for comparison (Fig. S3). PEG or dodecane were added to two tubes of GSNs suspensions followed by investigating the performance respectively. After modification with PEG or dodecane, the inhomogeneous solution was gained, and the resulted products aggregated and

precipitated in ODCB (Fig. S3a, b). In the mixture of ODCB and water, both the resulted PEG and dodecane products were extracted into the interface and water layers in the form of precipitation mostly (Fig. S3c, d), which illustrated that the covalent functionalization could not be achieved without the help of azides. Therefore, azide groups were the keys for the covalent functionalization of GSNs.

### **8. Stability tests of AGSN for Raman analysis**

To further investigate the stability of the AGSN, different concentrations of acid, alkali, salt, oxide and reductant were utilized. AGSNs and R6G were mixed in 50 mM NaIO<sub>4</sub>, 50 mM KMnO<sub>4</sub>, 50 mM NaBH<sub>4</sub>, 500 mM HNO<sub>3</sub>, 500 mM NaOH and 500 mM NaCl aqueous solution respectively. The peaks of R6G varied greatly especially in NaOH, NaIO<sub>4</sub> and KMnO<sub>4</sub>. In contrast, the Raman peaks around 1330, 1590 and 2640 cm<sup>-1</sup> of AGSNs all showed little changes, which demonstrated that GSN possessed superior stability even in intense environment. To investigate the dispersity of the AGSNs in various conditions, UV-vis spectrophotometer was utilized to monitor the dynamic dispersity of AGSNs in various conditions including acid, alkali, salt, oxidant and reductant. AGSNs were mixed in 50 mM NaIO<sub>4</sub>, 50 mM NaBH<sub>4</sub>, 500 mM HNO<sub>3</sub>, 500 mM NaOH and 500 mM NaCl solution for 20 min respectively. The surface plasmon resonance (LSPR) peaks around 400 nm and 600 nm of AGSNs in various conditions showed few changes, demonstrating the few aggregation and commendable dispersity of AGSNs even in intense environments (Fig. S6).

## **9. Raman analysis of AGSN as an internal standard**

5  $\mu\text{M}$  R6G was mixed with AGSN aqueous solution. Then more than six measurements were performed for every Raman spectrum in a Renishaw Invia Raman system with 633 nm laser. The original Raman spectra of R6G and AGSN mixed solution were obtained by changing the focusing depth and power of laser.

## **10. Preparation of fish samples**

About 100 g of frozen tilapia fillets (Guolian Aquatic Co., Ltd, Guangdong, China) was homogenized for 10 min and certified to contain no MG and LMG by an LC-MS/MS method.<sup>S-4</sup> Then tilapia homogenates were contaminated with LMG at levels of 2  $\mu\text{g g}^{-1}$ . The contaminated fish homogenates ( $1.00 \pm 0.01$  g) were mixed with 10 g  $\text{L}^{-1}$  (500  $\mu\text{L}$ ) hydroxylamine solution to prevent degradation of the LMG analytes, and kept at room temperature for 20 min before extraction. Then, the fish homogenates were extracted with 2 mL acetonitrile and water respectively, and followed by adding  $4.0 \pm 0.1$  g alumina to remove the lipids of fish. After that, the two kinds of supernatant in corresponding acetonitrile and water were obtained by centrifuging the solution. Next, LMG was oxidized to MG by adding DDQ and reacting for more than 5 min. The supernatant was then centrifuged and filtered through PVDF filter (0.4  $\mu\text{m}$ ) before SERS analysis.



## 11. Raman analysis of AGSN for LMG and MG in different solvents

In Fig. S7, the standard concentration curves of MG and LMG were obtained after mixing AGSN with different concentrations of MG and LMG in water and acetonitrile separately. For the detection of MG (LMG), we have calibrated the factors and chose the optimized experiment conditions. The utilized laser wavelength, laser power, integration time per pixel, concentrations of AGSNs in water and acetonitrile, were 633 nm, 100%, 3 seconds, 1.7 mg mL<sup>-1</sup> and 1.5 mg mL<sup>-1</sup>, respectively. Fig. S7a showed the original spectra of AGSN upon adding MG at different concentrations, in which the Raman peaks of 802 cm<sup>-1</sup> and 1330 cm<sup>-1</sup> belonged to MG and AGSN respectively. Fig. S7b showed the relative intensity of MG, i.e., ratio ( $I_{802}/I_{1330}$ ) with the D band of AGSN as the internal standard (regression coefficient  $R^2=0.9892$ ). The detectable limit for MG in water was 10 ng mL<sup>-1</sup>. Fig. S7c showed the original spectra of AGSN upon adding LMG at different concentrations. Fig. S7d showed the relative intensity of LMG, i.e., ratio ( $I_{802}/I_{1330}$ ) with the D band of AGSN as the internal standard (regression coefficient  $R^2=0.9894$ ). The detectable limit for LMG acetonitrile was 18 ng mL<sup>-1</sup>. All the measurements were carried at 25±1°C. The Raman spectra of MG, AGSN and acetonitrile were showed in Fig. S8, in which there were no overlap at the peaks of 802 cm<sup>-1</sup> and 1330 cm<sup>-1</sup>.

To certify the enhanced SERS performance of AGSNs in fluids, the SERS spectra of the analytes enhanced with AGSNs and bare GSNs were measured respectively (Fig. S9). When the bare GSNs acted as the SERS substrates, hardly any SERS signals at 802 cm<sup>-1</sup> were measured in the 100 ng mL<sup>-1</sup> MG and 540 ng mL<sup>-1</sup> LMG solutions. Such

weak SERS performance of bare GSNs was caused by the poor dispersity in liquids. However, with the AGSNs as the SERS substrates, the strong SERS signals were observed in the both fluids, which demonstrated that the covalent functionalization increased the dispersity of AGSNs while leading to the enhanced SERS performance in fluids.

## Supplementary Figures

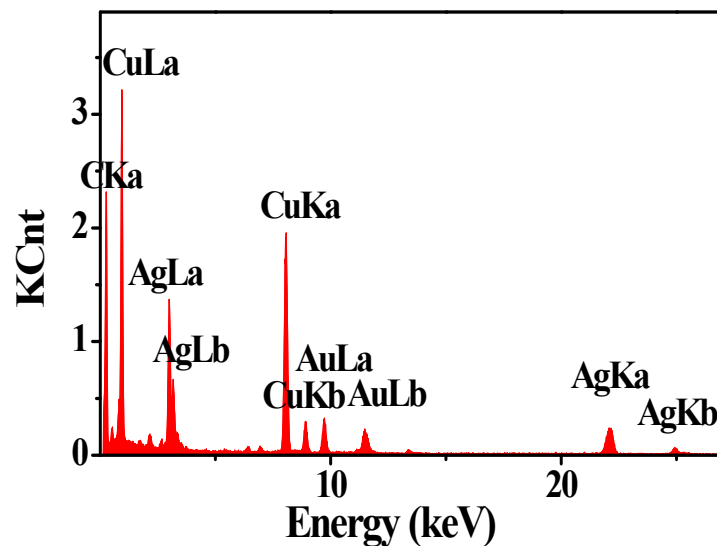


Fig. S1. Energy dispersive spectroscopy (EDS) of GSN.

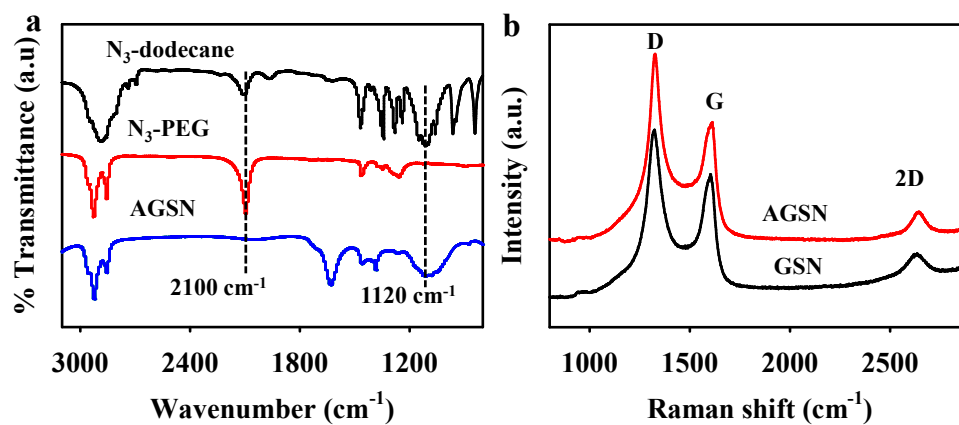
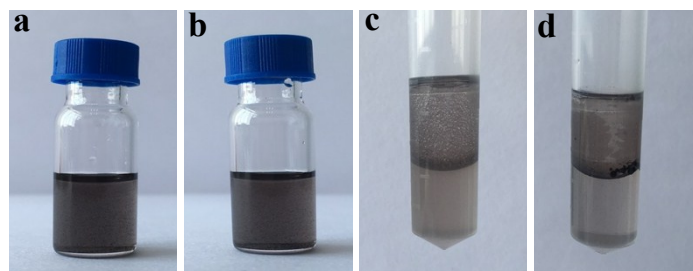
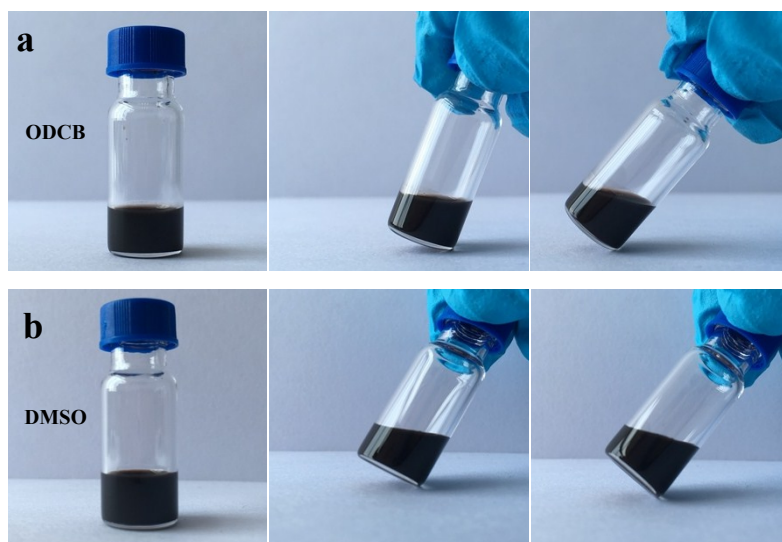


Fig. S2. (a) FT-IR spectra of N<sub>3</sub>-dodecane (black), N<sub>3</sub>-PEG (red) and AGSN (blue).

(b) Raman spectra of original GSN (black) and AGSN (red).



**Fig. S3.** Photos of GSNs treated with PEG and dodecane without azides. (a) Reaction mixture of GSNs treated with PEG (a) and dodecane (b) in ODCB. GSNs functionalized with PEG (c) and dodecane (d) in the mixed solvent of ODCB (bottom layer) and water (top layer).



**Fig. S4.** Photos of AGSNs dispersed in ODCB and DMSO with the concentrations at  $11.4 \text{ mg/mL}^{-1}$  and  $9.2 \text{ mg/mL}$ , respectively.

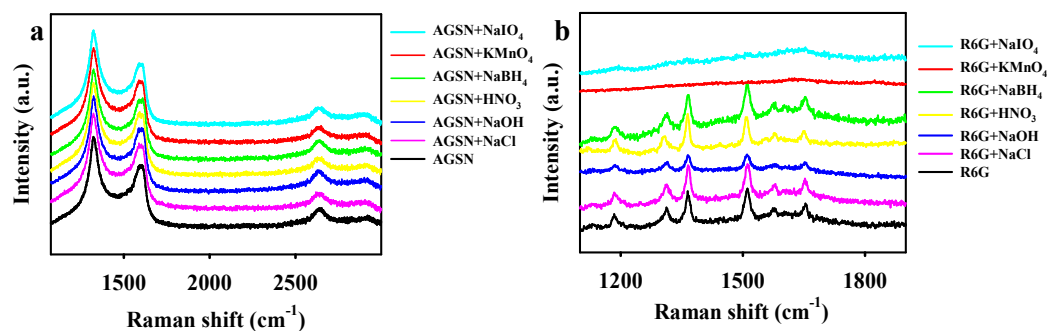


**Fig. S5.** Stability of AGSN. Raman spectra of AGSN (a) and R6G (b) mixed in 50 mM NaIO<sub>4</sub>, 50 mM KMnO<sub>4</sub>, 50 mM NaBH<sub>4</sub>, 500 mM HNO<sub>3</sub>, 500 mM NaOH and 500 mM NaCl aqueous solution respectively.

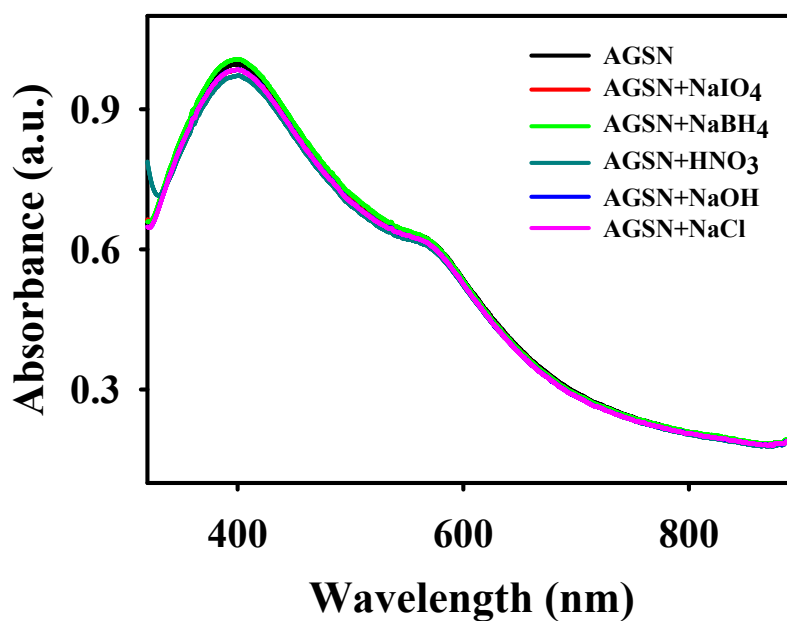


**Fig. S6.** The dispersity of AGSNs in various conditions. Uv-vis spectra of AGSNs mixed mixed in 50 mM NaIO<sub>4</sub>, 50 mM NaBH<sub>4</sub>, 500 mM HNO<sub>3</sub>, 500 mM NaOH and 500 mM NaCl solutions respectively.

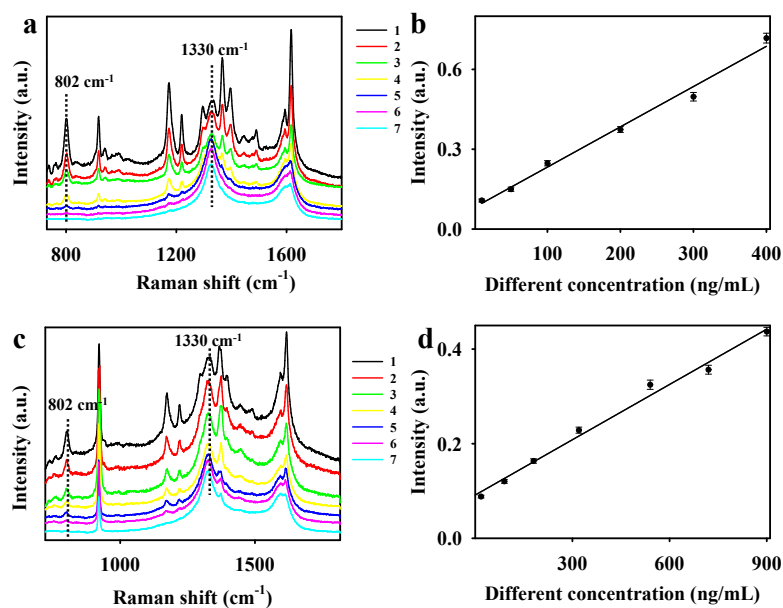


**Fig. S7.** (a) Raman spectra of various concentrations of MG mixed with AGSN in water (from line 1 to 7: 400, 300, 200, 100, 50, 20, 10 ng/mL). (b) Relative Raman intensity ( $I_{802}/I_{1330}$ ) vs. concentration of MG in water. (c) Raman spectra of various concentrations of LMG mixed with AGSN in acetonitrile (from line 1 to 7: 900, 720, 540, 320, 180, 90, 18 ng/mL). (d) Relative Raman intensity ( $I_{802}/I_{1330}$ ) vs. concentration of LMG in acetonitrile.

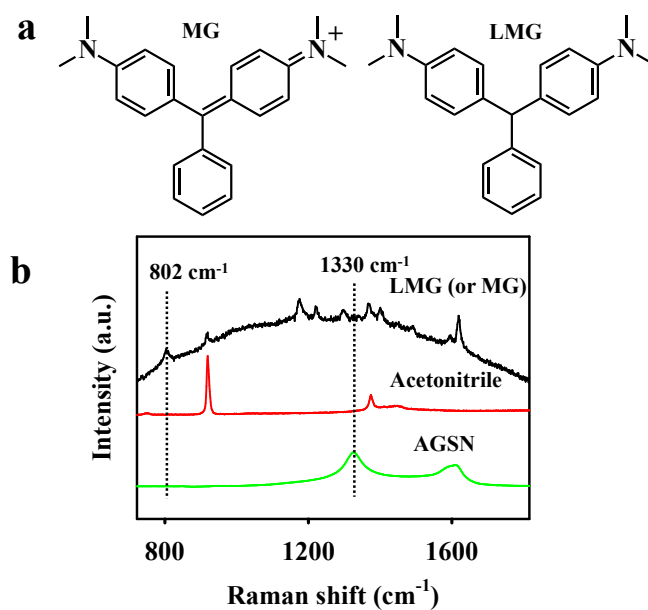


**Fig. S8.** (a) Chemical structure of MG and LMG molecules. (b) Raman spectra of MG, acetonitrile and AGSN.

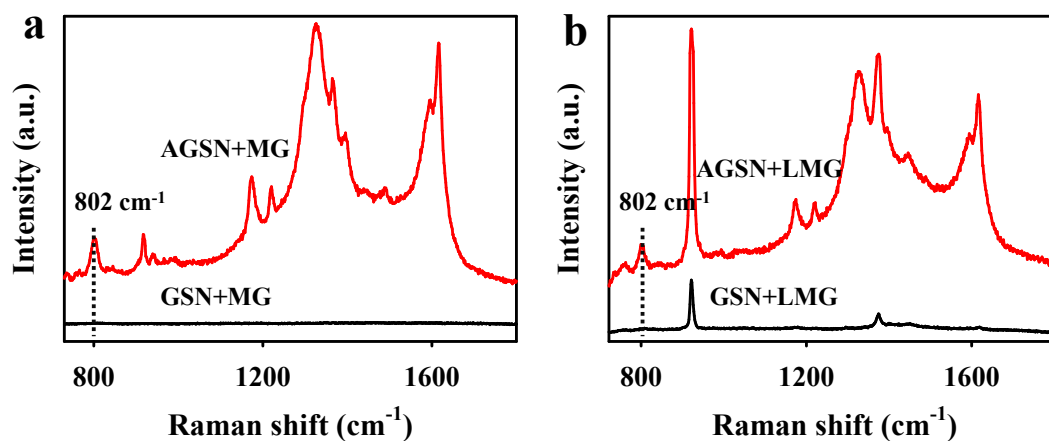


**Fig. S9.** (a) Raman spectra of 100 ng/mL MG enhanced with GSN and AGSN in water respectively. (b) Raman spectra of 540 ng/mL LMG enhanced with GSN and AGSN in acetonitrile respectively.

## References

- [S-1] Z. L. Song, Z. Chen, X. Bian, L. Y. Zhou, D. Ding, H. Liang, Y. X. Zou, S. S. Wang, L. Chen, C. Yang, X. B. Zhang and W. Tan, *J. Am. Chem. Soc.*, 2014, **136**, 13558-13561.
- [S-2] W. Guo, R. Pleixats, A. Shafir and T. Parella, *Adv. Synth. Catal.*, 2015, **357**, 89-99.
- [S-3] S. Lee, J. Hong, J. H. Koo, H. Lee, S. Lee, T. Choi, H. Jung, B. Koo, J. Park, H. Kim, Y. W. Kim, and T. Lee, *ACS Appl. Mat. Interfaces*, 2013, **5**, 2432-2437.
- [S-4] D. Hurtaud-Pessel, P. Couëdor and E. Verdon, *J. Chromatogr A*, 2011, **1218**, 1632-1645.